DRC-30

Backstepping Boundary Control for Vibration Suppression of the Undamped Shear Beam with Sliding base

Nipon Boonkumkrong[1*], Jirametha Sungkasem[2], Noppong Srithakul[3]

[1,2] Department of Mechanical Engineering, Faculty of Engineering, Kasem Bundit University,
1761 Pattanakarn Rd., Bangkok 10250, Thailand
[3] Department of Mechanical Engineering, Faculty of Engineering and Industrial Technology, Silpakorn University,
Sanam Chandra Palace campus, Rachamakka Nai Rd., Muang, Nakhon Pathom 73000, Thailand
*Corresponding Author: nipon413@hotmail.com

Abstract

This paper presents a backstepping boundary control for suppression of vibration of the mechanical systems. In this research, we use a shear beam with sliding base as a plant. The applications are such as space structure, industrial robotic arm etc. Most slender beams can be modeled using the shear beam. The shear beam is more complex than the conventional Euler-Bernoulli beam in that a shear deformation is additionally taken into account. The method allows us to deal directly with the beam's partial differential equations (PDEs) without resorting to approximations. An observer is used to estimate the deflections along the beam. Gain kernel of the system is calculated and then used in the control law. The control set-up is anti-collocation. Finite difference equations are used to solve the PDEs and the partial integro-differential equations (PIDEs). Numerical results for the control of a shear beam are presented via computer simulation to verify that the control scheme is effective. Control parameters are also varied to see their influences that affect the control performance.

Keywords: Backstepping boundary control, Shear beam, Partial differential equations, Gain kernels, Observer, Finite difference equations

1. Introduction

Flexible beams constitute an important problem in many applications such as space structures, industrial robotic arms, cantilever cranes, helicopter rotor, astronomical telescopes, the atomic force microscope (AFM) in nanotechnology devices etc. In this paper, we consider a model of the undamped shear beam. Most of the slender beams can be represented by this model. The beam system is distributed parameter in nature, so it's governed by partial differential equations (PDEs). The model consists of a wave equation coupled with a second-order-in-space ODE or can be alternatively represented as a fourth-order-in-space/second order-in-time PDE. The shear beam is more complex than the Euler–Bernoulli model and slightly simpler than the Timoshenko model. There are many models

for flexible beams such as Euler-Bernoulli, Rayleigh, shear and Timoshenko beam equations. Derivations and comparisons of these beam models can be found in [1].

Boundary control is preferable for controlling PDE systems since actuation and sensing are only through the boundary conditions [2]. For its historical development, the reader is referred to [3]. Morgul presented results for boundary control of infinite dimensional systems of Euler-Bernoulli [4]. The passivity property of nonlinear Euler-Bernoulli beams has been studied in Fard [5]. The method guarantees finite gain L_2 stability and passivity of closed-loop systems. Sasaki [6] used a Lyapunov functional of the system to derive the control law by minimizing the time rate of change of the functional at every point in time and using neural networks in tuning a control gain.

Krstic et al. presented the backstepping boundary control for undamped shear beams with an anticollocated setup i.e. the sensing and the actuation are at different locations [7, 8, 9, 10]. Gain kernels for both controller and observer are found and used for control law design. The application is such as atomic force microscopy (AFM) where the piezo actuation is applied at the beam base. The industrial application is rather limited. Ali and Padhi presented active control of Euler-Bernoulli beams [11]. They proposed two state feedback controllers based on optimal dynamic inversion techniques. Boonkumkrong N. and Kuntanapreeda S. applied the method of backstepping boundary control to the thermal system experiment [12].

This work is motivated by the interests in stabilizing vibrating slender bodies. The structure is modeled by a completely undamped shear beam model. The design is a combination of the classical damping boundary feedback idea with backstepping boundary control. The works of Fard, Sasaki and Krstic are the inspiration of this paper [5, 6, 7].

At present, the application of the backstepping boundary control is rather limited, due to the application of controllers to the beam is difficult. An objective of this paper is to apply the method to the problem of the free vibration suppression of the undamped shear beam with controllers applied to the beam by using sliding base. This is new method to apply the backstepping boundary controllers to the system.

The rest of this article is organized as follows. Next section presents a mathematical model of the system. Brief explanations of the beam models are also provided. Backstepping boundary controller design is given in Section 3. In Section 4, an observer design is present. Numerical studies are presented in Section 5. The results of simulation are given in Section 6. This article is concluded in the last section.

2. Mathematical model

The undamped shear beam model can be expressed by a second-order-in-time fourth-order-in-space PDE, as follows [1]

$$a\, w_{tt}(x,t) - \varepsilon\, w_{xxtt}(x,t) + w_{xxxx}(x,t) = 0 \qquad (1)$$

where $w(x,t)$ is the beam deflection, ε is a constant inversely proportional to the shear modulus and a is a positive constant. The subscripts t and x denote the partial differentiation with respect to time and space,

respectively. The deflection due to the mass of beam is neglected.

The beam model can be also represented by a wave equation PDE coupled with a second-order-in-space ODE as follows [1,14],

$$\varepsilon w_{tt}(x,t) = w_{xx}(x,t) - \varphi_x(x,t), \quad x \in (0,1) \qquad (2)$$

$$\varphi_{xx} - b^2\varphi + b^2 w_x = 0, \qquad (3)$$

where φ is the rotating angle as a result of the bending moment of the beam and $b = \sqrt{a/\varepsilon}$. The derivations of beam models Eq. (1) and Eqs. (2) - (3), can be found in [14]. In [14], one can verify that both models are equivalent.

In Fig. 1, the beam is free at one end $(x=0)$ and has the following boundary conditions [1],

$$w_x(0,t) - \varphi(0,t) = 0 \qquad (4)$$

$$\varphi_x(0,t) = 0. \qquad (5)$$

Eq. (4) and Eq. (5) mean that the shear force and the moment are both zero at the free end, respectively. The boundary condition of the other end $(x=1)$ with a controller, $U(t)$ to be designed, is as follows [6],

$$m_b \frac{d^2W(t)}{dt^2} = -\left(w_x(1,t) - \varphi(1,t)\right) + U(t), \qquad (6)$$

where m_b is the mass of sliding base, $W(t)$ is the displacement of the base, the terms in the parentheses on the right-hand side of Eq. (6) is a shear force exerts on the base [4]. The beam model, Eqs. (2) - (3) is used to design the control law. Note that $W(t) = w(1,t)$.

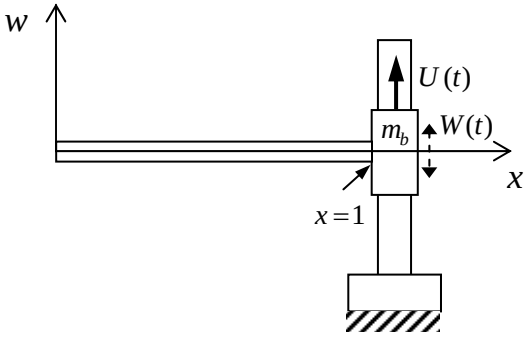

Fig. 1 Shear beam with a controller, $U(t)$

3. Backstepping Boundary Control

In this section, backstepping boundary control method is presented. Control law is then formulated.

3.1 Backstepping Boundary Control Design

The system, Eqs. (2) - (3), will be first re-written in a hyperbolic partial integro-differential equation (PIDE) as the following,

$$\begin{aligned}\varepsilon w_{tt}(x,t) &= w_{xx}(x,t) + b^2 w(x,t) - b^2\cosh(bx)w(0,t) \\ &+ b^3\int_0^x \sinh\left[b(x-y)\right] w(y,t)\,dy \\ &- \frac{b\cosh(bx)}{\cosh(b)}\left\{\begin{array}{l}\varphi(1,t) - b\sinh(b)\,w(0,t) \\ + b^2\int_0^1 \cosh\left[b(1-y)\right] w(y,t)\,dy\end{array}\right\}\end{aligned} \qquad (7)$$

$$\begin{aligned}w_x(0,t) = \frac{1}{\cosh(b)}\{&\varphi(1,t) - b\sinh(b)\,w(0,t) \\ &+ b^2\int_0^1 \cosh[b(1-y)]\,w(y,t)\,dy\}.\end{aligned} \qquad (8)$$

Eq. (7) and (8) are obtained by solving the ODE Eq. (3) as a two point boundary value problem using Laplace transform in the spatial variable x as follows [7]

$$\begin{aligned}\varphi(x,t) = &\cosh(bx)\,\varphi(0,t) \\ &- b\int_0^x \sinh\left(b(x-y)\right) w_y(y,t)\,dy.\end{aligned} \qquad (9)$$

The term $\varphi(0,t)$ in Eq. (9) can be expressed in term of $\varphi(1,t)$ by evaluating Eq. (9) at $x=1$ to get

$$\varphi(1,t)=\cosh(b)\,\varphi(0,t) - b\int_0^1 \sinh(b(1-y))\,w_y(y,t)\,dy \tag{10}$$

Solve Eq. (10) for $\varphi(0,t)$,

$$\varphi(0,t)=\frac{1}{\cosh(b)}\{\varphi(1,t) + b\int_0^1 \sinh(b(1-y))\,w_y(y,t)\,dy\} \tag{11}$$

Integrating by parts the integral term on the right side of Eq. (11) to get

$$\varphi(0,t)=\frac{1}{\cosh(b)}\{\varphi(1,t)-b\sinh(b)\,w(0,t) + b^2\int_0^1 \cosh(b(1-y))\,w(y,t)\,dy\} \tag{12}$$

The integral term on the right hand side of Eq. (12) is not spatially casual because the upper limit of integration is 1. To put the system into a strictly feedback form, we eliminate this integral by choosing the first controller as follows,

$$\varphi(1,t)=b\sinh(b)\,w(0,t) - b^2\int_0^1 \cosh(b(1-y))\,w(y,t)\,dy. \tag{13}$$

So that $\varphi(0,t)=0$ in Eq. (12). Then Eq. (9) becomes,

$$\varphi(x,t)=b\sinh(bx)\,w(0,t) - b^2\int_0^x \cosh(b(x-y))\,w(y,t)\,dy. \tag{14}$$

Note that the upper limit of integration is now x.

Differentiate $\varphi(x,t)$ with respect to x and substituting the results into the wave equation Eq. (2), we get the system in the strictly feedback form for control design,

$$\varepsilon\, w_{tt}(x,t)=w_{xx}(x,t)-b^2\cosh(bx)\,w(0,t) + b^3\int_0^x \sinh(b(x-y))\,w(y,t)\,dy. \tag{15}$$

$$w_x(0,t)=0. \tag{16}$$

Using the following transformation [7],

$$v(x,y)=w(x,y)-\int_0^x k(x,y)w(y,t)\,dy \tag{17}$$

to map the system Eq. (2) into the following exponentially stable target system

$$\varepsilon\, v_{tt}(x,t)=v_{xx}(x,t), \tag{18}$$

$$v_x(0,t)=c_0 v(0,t), \tag{19}$$

$$v_x(1,t)=-c_1 v_t(1,t) \tag{20}$$

where c_0 and c_1 are design parameters. Stability proof of Eq. (18) – (20) can be found in [9].

Substituting the transformation Eq. (17) into the target system, Eqs. (18) – (20), we can derive the following PDE for gain kernel $k(x,y)$ [13]:

$$k_{xx}(x,y)=k_{yy}(x,y)+b^2\sinh(b(x-y)) + b^3\int_0^x k(x,\xi)\,w(\xi,t)\,d\xi \tag{21}$$

$$k(x,x)=-\frac{\lambda}{2}x-c_0 \tag{22}$$

$$k_y(x,0)=b^2\int_0^x k(x,\xi)\cosh(b\xi)\,d\xi - b^2\cosh(bx) \tag{23}$$

The second boundary controller is obtained by differentiating Eq. (17) with respect to x and setting $x=1$: [13]

$$w_x(1,t)=k(1,1)\,w(1,t)+\int_0^1 k_x(x,y)\,w(y,t)\,dy - c_1 w_t(1,t)+c_1\int_0^1 k(1,y)\,w_t(y,t)\,dy \tag{24}$$

Stability proof of the feedback control can be found in [10]. Gain kernels $k(1,y)$ and $k_x(1,y)$ of

control law Eq. (24) are shown in Fig. 2 and Fig. 3, respectively.

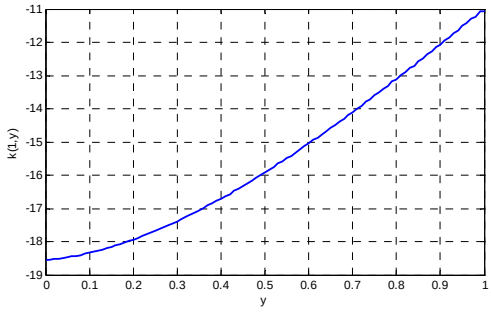

Fig. 2 The plot of the gain kernel $k(1, y)$.

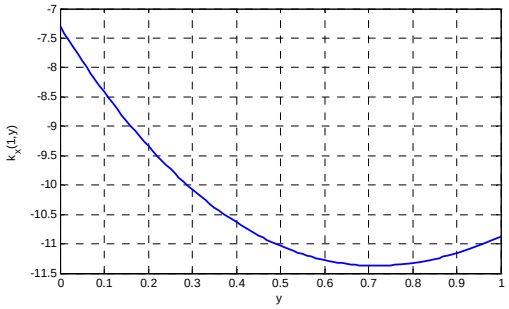

Fig. 3 The plot of the gain kernel $k_x(1, y)$.

In backstepping boundary control method, we use the controller, which consists of two equations i.e. Eq. (13) and Eq. (24) to control the beam. Fig. 4 shows the transformation from cantilevered beam to target system. The first part of controller, $\varphi(1,t)$ converts the free end into a sliding end i.e. $\varphi(0,t)=0$ and then the second part of the controller, $w_x(1,t)$, converts the beam into taut string with a stiff spring at the tip, Eq. (19) and a tuned damper at the base, Eq. (20).

The first controller, Eq. (13) is combined to the beam model, Eqs. (7) - (8), so the controller, Eq. (24) is applied at the sliding base as follows,

$$\begin{aligned} U(t) &= k(1,1)\,w(1,t) \\ &+ \int_0^1 k_x(x,y)\,w(y,t)\,dy - c_1 w_t(1,t) \\ &+ c_1 \int_0^1 k(1,y)\,w_t(y,t)\,dy \end{aligned} \qquad (25)$$

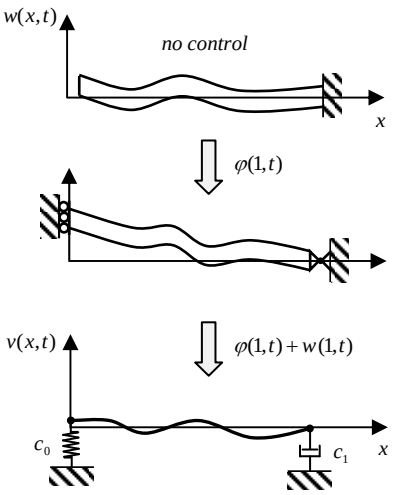

Fig. 4 Feedback transformation for beam.

4. Observer Design

For the backstepping boundary control method, the states along the beam is needed for control law calculation, but the only possible measurement of the system is at the boundary, $x=0$. The Luenberger-like observer is used to estimate beam deflections along the beam [10].

Consider the following beam model,

$$\begin{aligned} \varepsilon\, w_{tt}(x,t) &= w_{xx}(x,t) \\ &+ b^3 \int_0^x \sinh(b(x-y))\,w(y,t)\,dx \\ &- b^2 \cosh(bx)\,w(0) - b\sinh(bx)\,\alpha(0) \end{aligned} \qquad (26)$$

$$w_x(0,t) = \varphi(0,t) \qquad (27)$$

The Luenberger-like observer is given by [10]

$$\begin{aligned}\varepsilon\,\hat{w}_{tt}(x,t) &= \hat{w}_{xx}(x,t)+b^2\hat{w}(x,t)\\ &+b^3\int_0^x \sinh(b(x-y))\,w(y,t)\,dx\\ &-b^2\cosh(bx)\,w(0)-b\sinh(bx)\,\varphi(0)\\ &+p_y(x,0)\,[w(0,t)-\hat{w}(0,t)]\end{aligned} \tag{28}$$

$$\begin{aligned}\hat{w}_x(0,t) &= \varphi(0)+p(0,0)\,[w(0,t)-\hat{w}(0,t)]\\ &-\tilde{c}_0\,[w_t(0,t)-w_t(0,t)]\end{aligned} \tag{29}$$

$$\hat{w}(1,t)=w(1,t) \tag{30}$$

The observer gains $p_y(x,0)$ in Eq. (18) and $p(0,0)$ in Eq. (29) are determined by solving the PDE [10],

$$\begin{aligned}p_{yy}(x,y) &= p_{xx}(x,y)+b^2p(x,y)\\ &+b^3\sinh(b(x-y))\\ &+b^3\int_y^x p(\xi,y)\sinh(b(x-\xi))\,dx\end{aligned} \tag{31}$$

$$p(x,x)=\frac{b^2}{2}(x-1) \tag{32}$$

$$p(1,y)=0. \tag{33}$$

Defining the observer error as $\tilde{w}=w-\hat{w}$ and substracting Eqs. (28) - (29) from Eqs. (26) - (27) we obtain the observer error PDE,

$$\begin{aligned}\varepsilon\,\tilde{w}_{tt}(x,t) &= \tilde{w}_{xx}(x,t)+b^2\tilde{w}(x,t)\\ &+b^3\int_0^x \sinh(b(x-y))\,\tilde{w}(y,t)\,dx\\ &+p_y(x,0)\,\tilde{w}(0,t)\end{aligned} \tag{34}$$

$$\tilde{w}_x(0,t)=-p(0,0)\,\tilde{w}(0,t)+\tilde{c}_0\,\tilde{w}_t(0,t) \tag{35}$$

$$\tilde{w}(1,t)=0. \tag{36}$$

Using the following transformation,

$$\tilde{w}(x,t)=\tilde{v}(x,t)-\int_0^x p(x,y)\,\tilde{v}(y,t)dy \tag{37}$$

to convert the error system Eqs. (34) - (36) into

$$\varepsilon\,\tilde{v}_{tt}(x,t)=\tilde{v}_{xx}(x,t) \tag{38}$$

$$\tilde{v}_x(0,t)=\tilde{c}_0\,\tilde{v}_t(0,t) \tag{39}$$

$$\tilde{v}(1,t)=0, \tag{40}$$

which is known to be exponentially stable, see [10].

The gain kernel PDEs can be solved either numerically or recursively, but in this paper, we solve them numerically. The plot of observer gain kernel $p(x,1)$ and $p_y(x,1)$ are shown in Fig. 5 and Fig. 6, respectively.

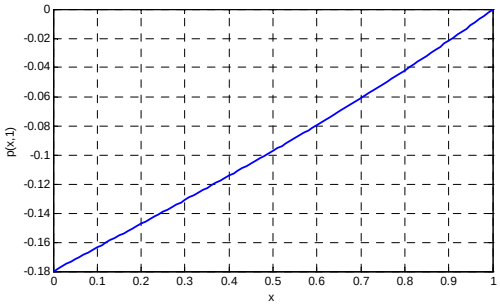

Fig. 5 The plot of the observer gain kernel $p(x,1)$.

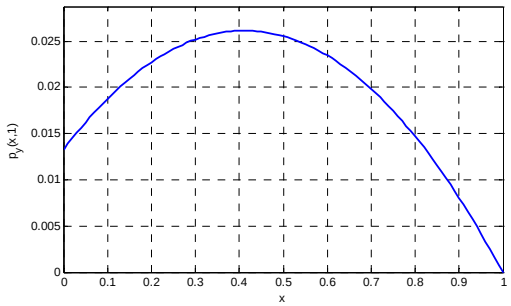

Fig. 6 The plot of the observer gain kernel $p_y(x,1)$.

5. Numerical Calculation

The beam model with strictly feedback form, Eq. (15) is a second-order-in-time second-order-in-space partial integro-differential equation (PIDE) and is used in a numerical calculation. It is a simple second-order partial differential equation

with the integration terms, and can be easily solved by a finite difference equation.

The highest order of the PIDE that we study in this paper is second order, so we have the following finite difference approximations [15]:

$$\left(\frac{\partial^2 w}{\partial x^2}\right)_m^n = \frac{w_{m+1}^n - 2w_m^n + w_{m-1}^n}{(\Delta x)^2} + O[(\Delta x)^2] \quad (41)$$

$$\left(\frac{\partial^2 w}{\partial t^2}\right)_m^n = \frac{w_m^{n+1} - 2w_m^n + w_m^{n-1}}{(\Delta t)^2} + O[(\Delta t)^2] \quad (42)$$

For the integration approximation, we use the trapezoidal integration rule as follows,

$$\int_a^b f(x)\,dx = \frac{\Delta x}{2} f(a) + \sum_{i=a+1}^{b-1} f(i) + \frac{\Delta x}{2} f(b) \quad (43)$$

Substituting Eqs. (41) – (43) into Eq. (15), we get the following finite difference equation,

$$\begin{aligned} w_m^{n+1} &= \frac{r^2}{\varepsilon}(w_{m+1}^n - 2w_m^n + w_{m-1}^n) + 2w_m^n - w_m^{n-1} \\ &+ \frac{(\Delta t)^2}{\varepsilon} b^2 w_m^n - \frac{(\Delta t)^2}{\varepsilon} b^2 \cosh(b\,x(m))\, w_1^n \\ &+ \frac{(\Delta t)^2}{\varepsilon} b^3 \left\{ \begin{array}{l} \frac{\Delta x}{2}\sinh[b(x(m) - y(1))]w(1) + \\ \Delta x \sum_{j=2}^{m-1} \sinh[b(x(m) - y(j))]w(j) \end{array} \right\} \end{aligned} \quad (44)$$

Where Δx and Δt are the spatial and the temporal increments indexed by m and n, which start from 1 to M and N, respectively and $r = \Delta t / \Delta x$ Fig. 7 shows the calculation grid with spacing Δx in the row and Δt in the column. The dark circles (the first and second rows from the bottom) are the values obtained by the initial conditions and the grey circle (w_m^{n+1}) is the point to be calculated.

With the boundary condition, Eq. (16), one can obtain the first element (w_1^{n+1}) of each row and from the controller, Eq. (25) and the boundary conditions Eq. (6), the last element of the row (w_M^{n+1}) is obtained.

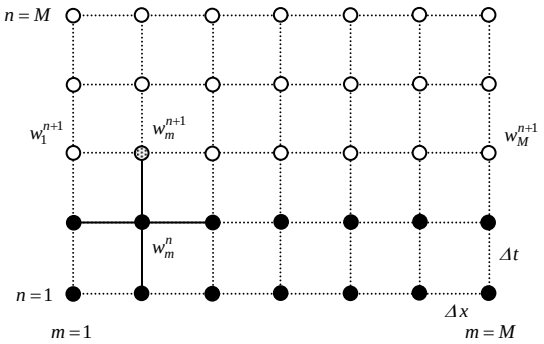

Fig. 7 Calculation grid

6. Simulation

In this section, the simulation results are presented. The shear beam is simulated using the finite difference equations mentioned in the last section. The beam started to vibrate under the following initial conditions (see Fig. 8) [8]:

$$w(x,0) = 0.1(1-x)^2 \sin(1.6\pi(1-x)) \quad (45)$$

$$w_t(x,0) = -0.1(1-x)^2 \sin(1.6\pi(1-x)), \quad (46)$$

where Eq. (45) is the initial displacement, and Eq. (46) is the initial velocity at $t = 0$.

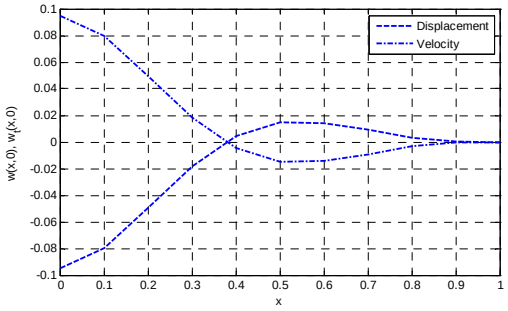

Fig. 8 Initial conditions

The beam was simulated with the parameter of beam material $\varepsilon = 1$ and $b = 0.6$. The mass of the sliding base was fixed at $m_b = 0.01$, and the

spring and damping constants were set at $c_0 = 1$ and $c_1 = 1$, respectively. The parameter for observer Eq. (29) is set at $\tilde{c}_0 = 15$ [8]. The grid size is $M = 20$ in space and time step $\Delta t = 0.01$ with final time $T = 30$ units. Since there is no damping term in the beam model, and also no external force exerted, the beam with zero Dirichlet boundary condition at $x = 1$ i.e. the slider is fixed, will vibrate perpetually as shown in Fig. 9. The tip displacement at $x = 0$ is shown in Fig. 10. This is the uncontrolled case.

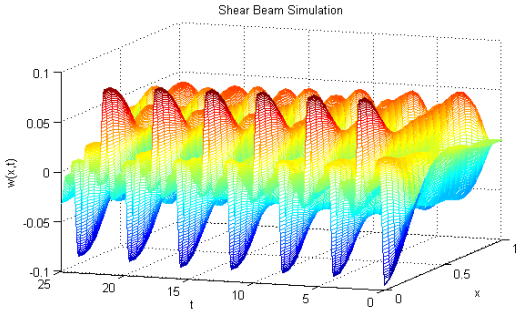

Fig. 9 Beam vibration without control in 3-D

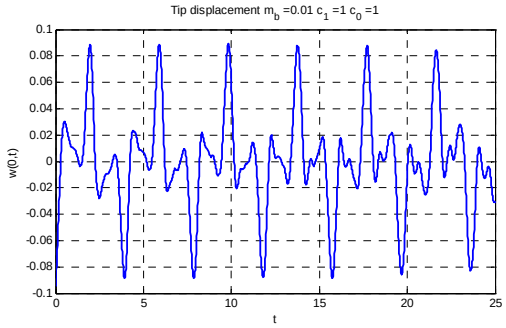

Fig. 10 Tip displacement of the Beam

The simulation of the shear beam with the control law, Eq. (25) is shown. The simulations of the shear beam with full-state control and with observer are shown in Fig. 11 and Fig.12, respectively. We see that the responses are the same. Note that the initial conditions for observer are 50% more than the values of Eq. (45) and Eq. (46).

The control action and tip displacement are shown in Fig. 13 and Fig. 14, respectively. The settling time is about $t = 20$.

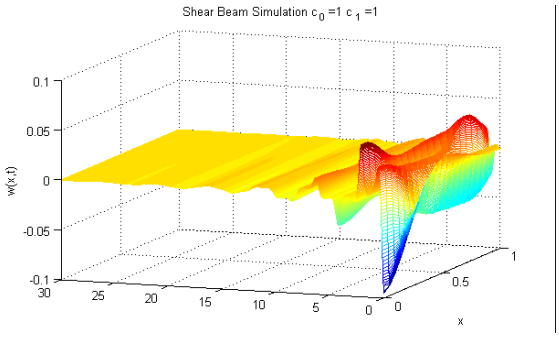

Fig. 11 Shear beam simulation with control

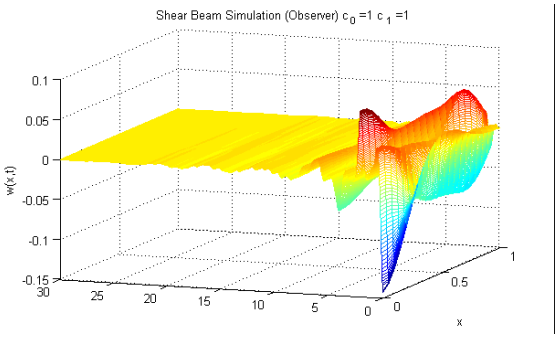

Fig. 12 Shear beam simulation with observer

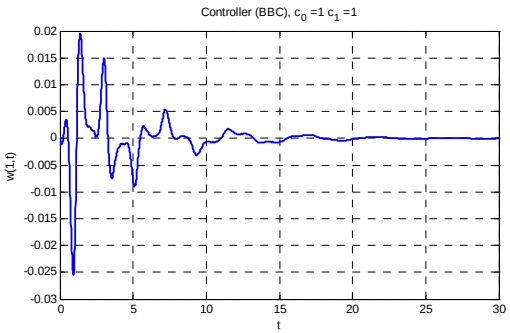

Fig. 13 Control action, $w(1,t)$.

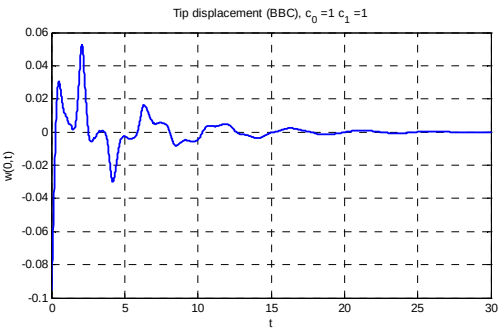

Fig. 14 Tip displacement, $w(0,t)$.

6.1 Parameter Tunings

In this sub-section, we study parameter changes that affect the control performance. First, we fix damping constant at $c_1 = 1.0$ and vary spring constants at various values, c_0 at 0.5, 1.0 and 2.0. Fig. 15 shows tip displacements.

In the case of a weak value of damping i.e. $c_0 = 0.5$, the response takes a longer time to settle at $t = 30$ and for the strong values of damping constant, it takes about $t = 20$.

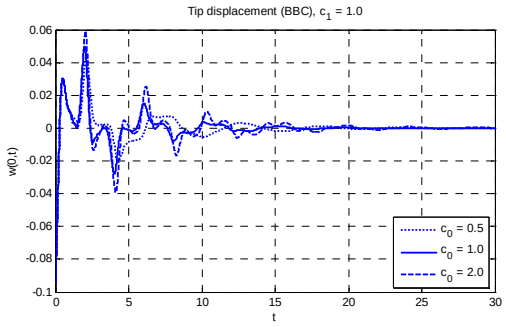

Fig. 15 Tip displacement with various spring constants (c_0).

In the second case, we fix spring constant at $c_0 = 1.0$ and in this time, we vary damping constants at various values, c_1 at 0.5, 1.0 and 2.0. Fig. 16 shows tip displacements of the beam. In the case of a weak value of damping i.e. $c_1 = 0.5$, the response takes a longer time to settle at $t = 30$ and for the strong values of damping constant, it takes about $t = 20$.

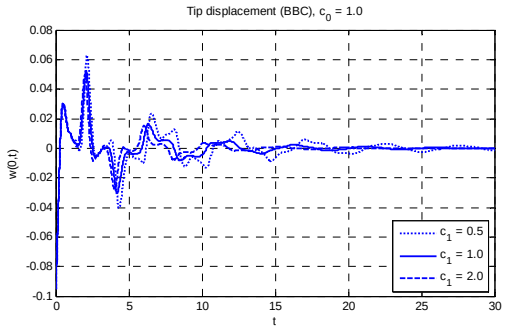

Fig. 16 Tip displacements with various damping constants (c_1).

7. Conclusion

Backstepping boundary control is applied to the problem of vibration suppression of the undamped shear beam. The beam model consists of a wave equation, coupled with a second-order-in-space ODE. An observer is used to estimate the deflections along the beam. Gain kernel of the system is calculated and then used in the control law. Finite difference equations are used to solve the PDEs and the partial integro-differential equations (PIDEs). Numerical results for the control of a shear beam are presented to verify that the control scheme is effective.

The control scheme is effective in suppressing the vibration of the beam, and the parameters, i.e. c_0 and c_1, can be tuned to obtain the control with the desired behaviors. For further research, the other boundary control methods such as passivity-based control method will be applied to the shear beam and their performance will be compared.

8. References

[1] Han S.M., Benaroya H. and Wei T. (1999), Dynamics of Transversely Vibrating beams using Four engineering Theories, *Journal of Sound and Vibration*, Vol. 225, 1999, pp. 935-988, 1999

[2] Smyshlyaev, A and Miroslav, M. (2004) Closed form boundary state feedbacks for a class of 1-D partial integro-differential equations, *IEEE Trans. On Automatic Control*, Vol. 49, No. 12, pp. 2185-2202, 2004.

[3] Padhi, R. and Ali, Sk F. (2009) An Account of Chronological developments in Control of Distributed Parameter Systems, *Annual reviews in Control 33*, pp. 59-68, 2009.

[4] Morgul O. (1992) Dynamic boundary control of the Timoshenko beam, *Automatica*, vol. 28, pp. 1255-1260, 1992.

[5] Fard, M.P., (2002) Passivity Analysis of Nonlinear Euler-Bernoulli Beams, *Modeling, Identification and Control*, Vol. 23, No. 4 pp. 239-258, 2002.

[6] Sasaki M., (2000) Asai H., Kawafuku M., and Hori Y., Self-tuning Control of a Translational Flexible arm using Neural networks, in *Proceedings of the IEEE International Conference on Systems, Man and Cybernetics*, pp. 3259-3264, Nashville, Tennessee, USA, October 2000.

[7] Krstic, M., Balogh, A. and Smyshlyaev, A., (2006) Backstepping Boundary Controller and Observer for the Undamped Shear Beam, *Proceedings of the 17th International Symposium on Mathematical Theory of Networks and Systems*, Kyoto, Japan, 24-28 July, 2006.

[8] Krstic M, Balogh A, and Smyshlyaev A, (2000) Backstepping Boundary Controllers for Tip-Force Induced Flexible Beam Instabilities Arising in AFM, *Proceedings of the 45th IEEE Conference on Decision & Control*, Manchester Grand Hyatt Hotel San Diego, CA, USA, 13-15 December, 2006

[9] Krstic M, Siranosian A, Balogh A. and Guo BZ, (2007) Control of Strings and Flexible Beams by Backstepping Boundary Control, *Proceedings of the 2007 American Control Conference*, Marriott Marquis Hotel at Times Square New York City, USA, 11-13 July, 2007

[10] Krstic M, Guo BZ., (2008) Control of A tip-force destabilized Shear beam by Observer-based Boundary feedback, *Journal of Control Optimization*, Vol. 47, No. 2, pp. 553–574, SIAM, 2008.

[11] Ali SF and Padhi R., (2009) Active vibration suppression of non-linear beams using optimal dynamic inversion. Proc IMechE, vol. 223 Part I: *Journal of Systems and Control Engineering*, pp. 657-672, 2009.

[12] Boonkumkrong N. and Kuntanapreeda S. (2014) Backstepping boundary control: An application to rod temperature control with Neumann boundary condition, Proc IMechE, vol. 228 Part I: *Journal of Systems and Control Engineering*, pp. 295-302, 2014.

[13] Krstic M., Smyshlyaev A.,"Boundary Control of PDEs: A Course on Backstepping Designs" SIAM, Philadelphia, PS 19104-2688 USA, 2008.

[14] Rao S.S., "Mechanical Vibrations", Third edition, Addison-Wesley Publishing Company, 1995.

[15] Mathews, J.H. and Fink, K.D. Numerical Methods Using MATLAB, Prentice Hall, Upper Saddle River, NJ 07458.